JOURNAL OF Materials CHEMISTRY

# A solvent-reduction and surface-modification technique to morphology control of tetragonal $In_2S_3$ nanocrystals†

**Yujie Xiong, Yi Xie,* Guoan Du and Xiaobo Tian**

*Structure Research Laboratory, Laboratory of Nanochemistry and Nanomaterials, University of Science and Technology of China, Hefei, Anhui, 230026, P. R. China.*
*E-mail: yxie@ustc.edu.cn*

***Received 21st June 2001, Accepted 15th October 2001***
***First published as an Advance Article on the web 26th November 2001***

$In_2S_3$ nanoparticles, short nanowhiskers, nanorods and finger-structure nanocrystals with stoichimetric composition and high quality can be prepared by a solvent-reduction route. It was found that the reagent concentrations, solvent and reaction temperature played important roles in the shape control. We also successfully used CTAB to modify the shape of products. The resulting structures were found to be quantum-confined.

## Introduction

A number of reviews have illustrated the continuing interest in III–VI compounds, and in particular $In_2S_3$ can be considered as a compound originating from II–VI semiconductors by substituting Group III elements for Group II elements.[1,2] Tetragonal indium sulfide, perhaps due to its defect structure, has attracted much attention for its optoelectronic properties,[3,4] electronic properties,[5,6] optical properties,[7] acoustic properties[8] and semiconductor sensitization[9] in recent years. It can be used as an n-type semiconductor with a medium energy gap of 2.00 eV,[10,11] as a photoconductor,[3,4] as a material in the preparation of green and red phosphors, and as a material in the manufacture of picture tubes for color televisions,[12,14] dry cells,[15] and heterojunctions for photovoltaic electric generators.[16]

Tetragonal $In_2S_3$ can be prepared by direct reaction of the elements,[17] heat treatment of $In_2O_3$ in $H_2S$,[18] metathesis reaction of solid $InCl_3$ and $Li_2S$,[19] or thermal decomposition of butylindium thiolates.[20] Solution preparation methods of indium sulfide have also been reported, such as aqueous metathesis reactions,[16,21,22] colloidal reaction in the presence of a polymer stabilizer,[23] and the injection method.[24] Our group also attempted to use a solvothermal route to prepare nanocrystalline tetragonal $In_2S_3$ at relatively low temperatures.[25,26] However, it is difficult to control the morphology of the products by this route.

It is well known that the particle sizes and shapes of tetragonal $In_2S_3$ are important for photoerosion of the material,[27,28] as well as in modifying the band gap.[16] Moreover, catalytic reactivity depends on the size and shape of the nanoparticles, and therefore the synthesis of well-controlled shapes and sizes of colloidal particles could be critical for their applications.[29] In terms of particle shapes Nittmann and Stanley were the first to report fractal structures.[30] Several methods have been used in recent years for the preparation of colloidal metal sols, such as the ultraviolet irradiation photoreduction route to Ag dendrites.[31] Some other methods have also been applied to control the morphology of metal sulfides, such as $FeS_2$,[32] MnS,[33] and ZnS.[34] To our knowledge, no report has been published concerning morphology control of nanocrystalline tetragonal $In_2S_3$. In this paper, we report a solvent-reduction and surface-modification technique for the preparation of single-crystalline tetragonal $In_2S_3$ short nanowhiskers, nanorods and finger-structure nanocrystals, similar to the theoretical structures reported by Nittmann.[30]

## Experimental

In a typical experimental procedure, the products were synthesized from stoichiometric mixtures of $InCl_3{\cdot}4H_2O$ and $Na_2S_2O_3{\cdot}5H_2O$. The reagent concentrations used to obtain the as-prepared products A, B, C, D and E were 0.01, 0.02, 0.04, 0.08 and 0.16 mol $L^{-1}$, respectively. The mixtures were loaded into a 50 ml Teflon-lined autoclave, which was then filled with absolute ethanol up to 90% of the total volume. The autoclave was then sealed and maintained at 180 °C for 24 h and was then cooled to room temperature naturally. The precipitate was filtered off, washed with absolute ethanol and distilled water several times, and then dried in vacuum at 60 °C for 4 h. In order to modify the shape of products, cetyltrimethylammonium bromide (CTAB) as a modifier was added to the autoclave at a concentration of 0.2 mol $L^{-1}$ with the other conditions kept constant.

X-Ray diffraction (XRD) patterns were collected on a Japan Rigaku D/max rA X-ray diffractometer equipped with graphite monochromatized high-intensity Cu-K$\alpha$ radiation ($\lambda$ = 1.54178 Å). The accelerating voltage was set at 50 kV, with 100 mA flux at a scanning rate of 0.06° $s^{-1}$ in the 2$\theta$ range 20–70°. Transmission electron microscopy (TEM) images and electronic diffraction (ED) patterns were taken on a Hitachi Model H-800 instrument with a tungsten filament, using an accelerating voltage of 200 kV. X-Ray photoelectron spectra (XPS) were collected on an ESCALab MKII X-ray photoelectron spectrometer, using non-monochromatized Mg-K$\alpha$ X-rays as the excitation source. UV–vis and photoluminescence (PL) spectra were recorded on a JGNA Specord 200 PC UV–vis spectrophotometer and Hitachi 850 fluorescence spectrophotometer, respectively.

## Results and discussion

The XRD patterns of typical samples of tetragonal $In_2S_3$ as prepared are shown in Fig. 1. All the reflections could be indexed to the tetragonal $In_2S_3$ phase with lattice parameters

†Electronic supplementary information (ESI) available: ED patterns of products C, D and E; XPS spectra: In 3d and S 2p core level spectra of $In_2S_3$. See http://www.rsc.org/suppdata/jm/b1/b105483j/

 DOI: 10.1039/b105483j

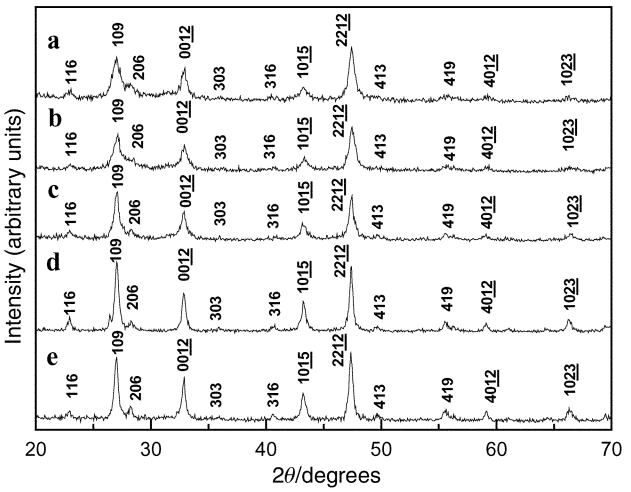


**Fig. 1** Powder XRD patterns of the samples: (a) product A; (b) product C; (c) product D; (d) product E.

$a = (7.613 \pm 0.002)$, $c = (32.326 \pm 0.005)$ Å, which are in agreement with the reported data of $a = 7.619$, $c = 32.329$ Å for $In_2S_3$ (JCPDS Card Files, 25-390). No characteristic peaks were observed for impurities such as $In_2O_3$, S or $In(OH)_3$. Using the Scherrer formula, the average sizes of products A, C, D and E were 15, 20, 30 and 30 nm, respectively.

Typical TEM images of as-prepared tetragonal $In_2S_3$ nanocrystals are shown in Fig. 2. It can be seen that the as-obtained $In_2S_3$ nanocrystals of products A, C, D and E are nanoparticles (15 nm), short nanowhiskers (20 nm × 200 nm), short nanorods (30 nm × 150 nm) and finger-structure nanocrystals (60 nm × 400 nm), respectively, which agreed with the average sizes from XRD. Some nanorods could also be found in product E. The TEM image of product B shows nanoparticles with a few short nanowhiskers (arrowed). Upon addition of the CTAB modifier, the morphologies of the as-prepared products were more regular. The products were nanoparticles (12 nm), longer nanowhiskers (18 nm × 750 nm) (Fig. 2(f); In and S reagent concentrations of 0.04 mol $L^{-1}$) and nanorods (50 nm × 1600 nm) (Fig. 2(g); In and S reagent concentrations of 0.08 mol $L^{-1}$), respectively. However for concentrations of $InCl_3{\cdot}4H_2O$ and $Na_2S_2O_3{\cdot}5H_2O$ of 0.16 mol $L^{-1}$ and added CTAB, no finger-structure nanocrystals, but rather nanorods were found. ED patterns (see electronic supplementary information†) show that the as-prepared short nanowhiskers, nanorods and finger-structure nanocrystals were tetragonal single crystals. The ED patterns of products C, D and E were square, square and rectangular, respectively, the rectangular pattern of product E being recorded along the *b* axis, while the square ones of products C and D were recorded along the *c* axis.

Further evidence for the quality and composition of the samples was obtained by XPS of the products. The binding energies obtained in the XPS analysis were corrected for specimen charging by referencing the C 1s signal to 284.60 eV. The In 3d core level spectrum shows the observed value of the binding energy for In $3d_{5/2}$ (444.3 eV) agrees with the reported data for $In_2S_3$ (444.3 eV).[35] The kinetic energy of the In $M_4N_{45}N_{45}$ peak is 408.0 eV. Therefore the value of the "modified Auger parameter" ($a'$) is 852.3 eV, which is in agreement with the literature value for $In_2S_3$ but clearly distinct from that for $In_2O_3$.[35] The S $2p_{3/2}$ binding energy of $In_2S_3$, centered at 161.6 eV, is very similar to that observed in chalcopyrite $CuFeS_2$.[36] The contents of In and S were quantified by In 3d and S 2p peak areas, and a molar ratio of 1 : 1.46 for In : S was found. No obvious peaks for elemental sulfur or other impurities were observed. Thus XPS analysis shows the products are pure $In_2S_3$ and contain no oxide impurities.

In the solvent-reduction process, the concentrations of the reagents $InCl_3{\cdot}4H_2O$ and $Na_2S_2O_3{\cdot}5H_2O$ are found to play a significant role in the shape control of the as-prepared products. We can see that the shape of the products changed from nanoparticles, short nanowhiskers, nanorods to finger-structure nanocrystals with an increase of the reagent concentrations. The TEM image of product B (Fig. 2(b)) is a good example showing the change of nanocrystal shapes. It is obvious that an increase of the reagent concentrations is helpful to obtain products of diffusion-limited aggregation (DLA). It is interesting that we obtained finger-structure nanocrystals when the reagent concentrations were increased to 0.16 mol $L^{-1}$. This large, new, random supramolecular structure of tetragonal $In_2S_3$ nanoparticles represents a very wide variety of growth, in which one particle after the other is formed and then diffuses and sticks to the growing structure.[30] The resulting structures are similar to the viscous finger structures reported by Nittmann.[30]

Ethanol is believed to act as a reducing agent, able to reduce $In^{3+}$ to elemental In. The reaction mechanism can be described in terms of eqns. (1)–(3):

$$2In^{3+} + 3CH_3CH_2OH \xrightarrow{180\,^{\circ}C} 2In + 3CH_3CHO + 6H^+ \quad (1)$$

$$S_2O_3{}^{2-} + 2H^+ \rightarrow S + SO_2 + H_2O \quad (2)$$

$$2In + 3S \xrightarrow{180\,^{\circ}C} In_2S_3 \quad (3)$$

The temperature of 180 °C and consumption of $H^+$ in eqn. (2) promotes the reduction of $In^{3+}$. This mechanism was established in separate experiments: on substituting elemental S for $Na_2S_2O_3$ tetragonal $In_2S_3$ was obtained; when $Na_2S$ was used, neither tetragonal $In_2S_3$ nor $In(OH)_3$ were found in the as-prepared products, which indicates the whole process was an elemental-reaction route. The IR spectrum of the solvent after reaction also showed eqn. (1) was reasonable: an absorption peak at 1741 $cm^{-1}$ which corresponds to the C=O stretching vibration of $CH_3CHO$ was observed. In the reaction process, produced In would be a liquid when the reaction temperature was 180 °C, above the melting point of In (157 °C).[37] The existence of liquid In may aid reaction leading to the growth of $In_2S_3$ short nanowhiskers and nanorods. This mechanism resembles that of the complex solution–liquid–solid (SLS) process proposed for the growth of InP whiskers by the group of Trentler and Buhro,[38,39] where the elements of the crystal phase are fed from a solution phase and pseudo-one-dimensional growth of the crystal phase from the flux liquid In after supersaturation is achieved. As for finger-structure nanocrystals, this is a type of fractal probably resulting due to molecular anisotropy and non-equilibrium growth.[30,40] The appearance of an In flux may lead to such factors.

In the surface-modification process, CTAB could adhere to the produced In flux, due to the electrostatic attraction between $C_{16}H_{33}(CH_3)_3N^+$, $Br^-$ and $In^{3+}$, as illustrated in Scheme 1.[41,42] It is obvious that this procedure can modify the surface of products and reduce vertical diffusion of the In flux. Therefore, the as-prepared nanowhiskers and nanorods were longer than those without CTAB modification. It is interesting that no finger-structure nanocrystals were found in the products with CTAB modification. In order to investigate the modifying effect of CTAB, we substituted sodium dodecyl sulfate (SDS) for CTAB. In this instance no obvious modifying effect was observed since SDS preferably binds $Na^+$ and so excludes $In^{3+}$.

It is also found that reaction temperature plays a key role in the shape control of $In_2S_3$ nanocrystals. At too low temperatures, the aggregation of nanoparticles to complicated

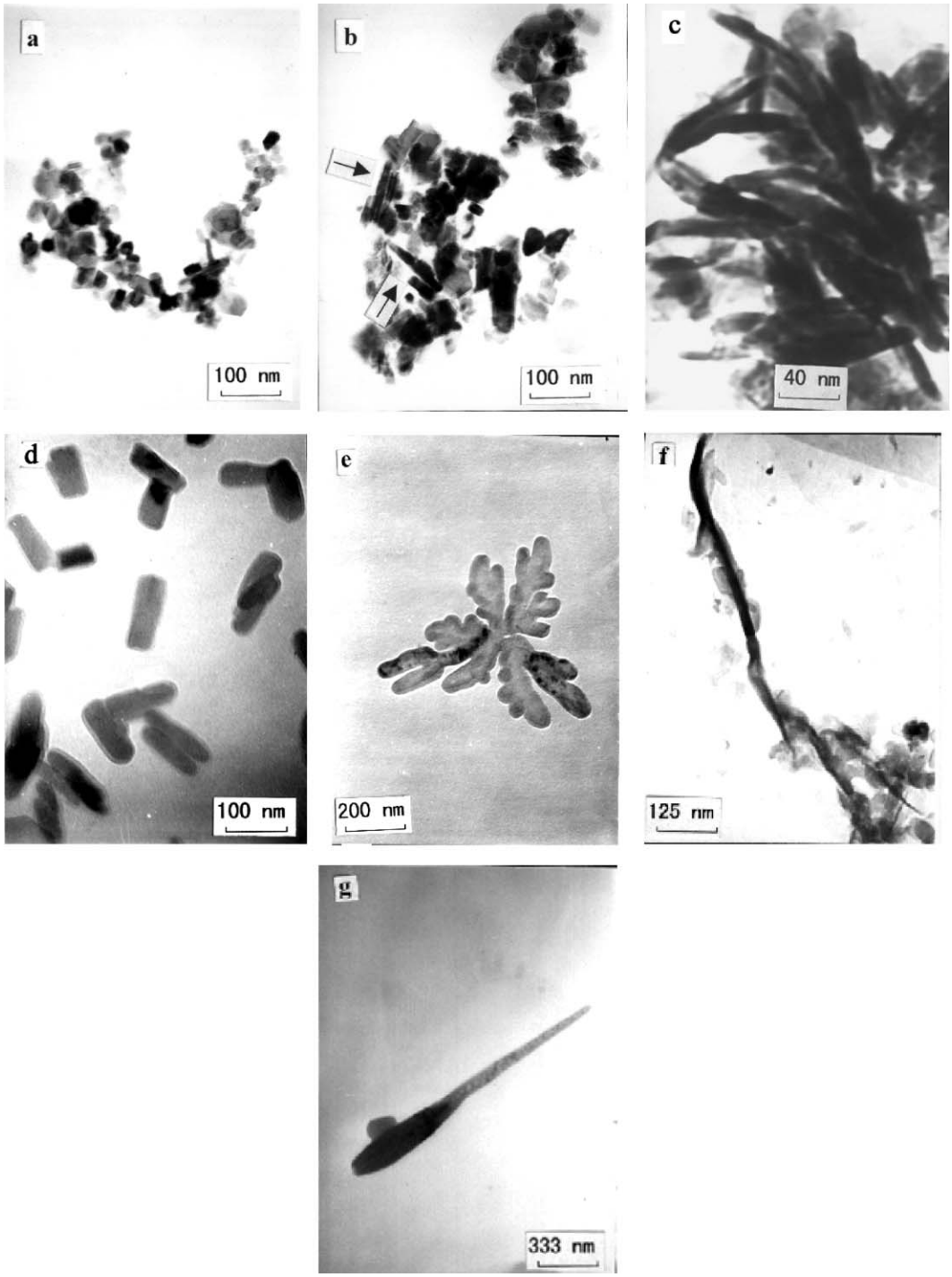


**Fig. 2** TEM images of the samples: (a) product A, nanoparticles; (b) product B, nanoparticles with a few short nanowhiskers; (c) product C, short nanowhiskers; (d) product D, short nanorods; (e) product E, finger-structure nanocrystals; (f) nanowhiskers, product upon CTAB modification; (g) nanorods, product upon CTAB modification.

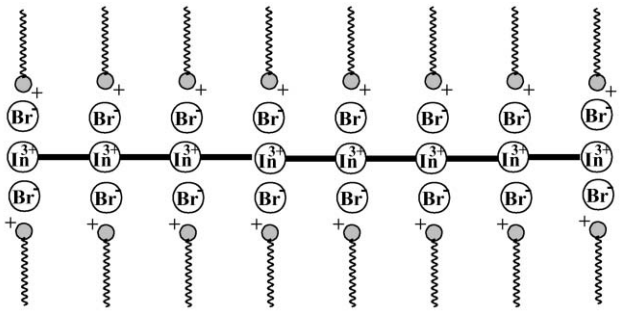

**Scheme 1**

structures and the presence of solid rather than liquid In are disadvantageous. At too high temperatures the nanoparticles readily aggregate to micrometer sized spheres. The optimum temperature was found to be 180 °C.

To examine the quantum-confined effect of the products, room-temperature UV–vis spectra and PL spectra were recorded with ethanol used as a reference. The results of UV–vis spectroscopy (Fig. 3) show that there are obvious absorption peaks of $In_2S_3$ nanoparticles, nanowhiskers, nanorods and finger-structure nanocrystals at 280, 320, 402 and 420 nm, respectively. It is obvious that there is a blue shift compared to reported data (620.6 nm) for $In_2S_3$ bulk materials,[3,4] which indicates the $In_2S_3$ nanoparticles, nanowhiskers,

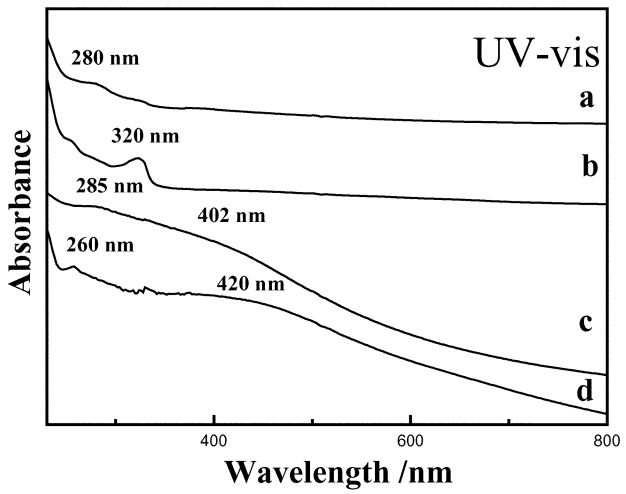


**Fig. 3** UV–vis spectra of the samples: (a) product A; (b) product C; (c) product D; (d) product E.

nanorods and finger-structure nanocrystals are quantum-confined. The larger differences between the peak and the onset in Fig. 3(b), (c) and (d), which might be related to the width of particle size distribution, are characteristic for nanowhiskers, nanorods and finger-structure nanocrystals. The width of absorption peaks and the other peaks at 260–285 nm in Fig. 3(c) and (d), which are in agreement with the absorption peak in Fig. 3(a), are probably caused by the different sizes of nanocrystals. Fig. 4(a) shows the PL excitation spectrum of product E while Fig. 4(b) is that of the reference ethanol. Under PL excitation at 260 nm, the finger-structure nanocrystals emit blue light at 358 nm, about 180 nm blue shifted compared with bulk $In_2S_3$.[43] This indicates quantum-confined effects of the $In_2S_3$ finger-struture nanocrystals.

## Conclusion

$In_2S_3$ nanoparticles, short nanowhiskers, nanorods and finger-structure nanocrystals with stoichimetric composition and high quality can be prepared by a solvent-reduction route. To our knowledge, no report has been published concerning the shape control of tetragonal $In_2S_3$. It is found the reagent concentrations, solvent and reaction temperature played important roles in the shape control. We also successfully used CTAB to modify the shape of the products which were found to be quantum-confined. This method may be extended to prepare novel nanostructures of other materials.

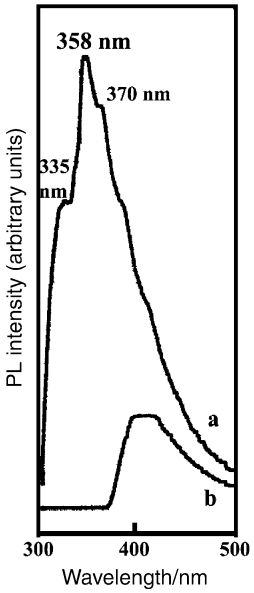


**Fig. 4** PL spectra: (a) product E; (b) ethanol reference.

## Acknowledgements

Financial support from the National Natural Science Foundation of China and Chinese Ministry of Education are gratefully acknowledged. We also thank Dr Jianping Xiao and Dr Xuchuan Jiang for their helpful suggestions for our paper.

## References

1 S. Suh and D. M. Hoffman, *Chem. Mater.*, 2000, **12**, 2794.
2 C. D. Lokhande, A. Ennaoui, P. S. Patil, M. Giersig, K. Diesner, M. Muller and H. Tributsch, *Thin Solid Films*, 1999, **340**, 18.
3 W. T. Kim and C. D. Kim, *J. Appl. Phys.*, 1986, **60**, 2631.
4 R. Nomura, S. Inazawa, K. Kanaya and H. Matsuda, *Appl. Organomet. Chem.*, 1989, **3**, 195.
5 N. Kamoun, S. Belgacem, M. Amlouk, R. Bennaceur, J. Bonnet, F. Touhari, M. Nouaoura and L. Lassabatere, *J. Appl. Phys.*, 2001, **89**, 2766.
6 A. A. El Shazly, D. Abd Elhady, H. S. Metwally and M. A. M. Seyam, *J. Phys. Condens. Matter*, 1998, **10**, 5943.
7 S. H. Choe, T. H. Bang, N. O. Kim, H. G. Kim, C. I. Lee, M. S. Jin, S. K. Oh and W. T. Kim, *Semicond. Sci. Technol.*, 2001, **16**, 98.
8 M. Amlouk, M. A. Ben Said, N. Kamoun, S. Belgacem, N. Brunet and D. Barjon, *Jpn. J. Appl. Phys., Part 1*, 1999, **38**, 26.
9 Y. Yasaki, N. Sonoyama and T. Sakata, *J. Electroanal. Chem.*, 1999, **469**, 116.
10 W. Rehwald and G. Harbeke, *J. Phys. Chem. Solids*, 1965, **26**, 1309.
11 J. M. Gilles, H. Hatwell, G. Offergeld and J. van Cakenberghe, *Phys. Status Solidi B*, 1962, **2**, K73.
12 Jpn. Pat. Appl., *Chem. Abstr.*, 1979, **91**, 67384a.
13 Jpn. Pat. Appl., *Chem. Abstr.*, 1979, **96**, 113316h.
14 Jpn. Pat. Appl., *Chem. Abstr.*, 1981, **95**, 107324x.
15 E. Dalas and L. Kobotiatis, *J. Mater. Sci.*, 1993, **28**, 6595.
16 E. Dalas, S. Sakkopoulos, E. Vitoratos and G. Maroulis, *J. Mater. Sci.*, 1993, **28**, 5456.
17 C. Kaito, Y. Saito and K. Fujita, *J. Cryst. Growth*, 1989, **94**, 967.
18 H. B. Richard and H. M. William, *J. Phys. Chem. Solids*, 1959, **10**, 333.
19 J. C. Fitzmaurice and I. P. Parkin, *Main Group Met. Chem.*, 1994, **17**, 481.
20 R. Nomura, S. Inazawa, K. Kanaya and H. Matsuda, *Appl. Organomet. Chem.*, 1989, **3**, 195.
21 M. F. Stubbs, J. A. Schufle, A. J. Thompson and J. M. Duncan, *J. Am. Chem. Soc.*, 1952, **74**, 1441.
22 P. N. Kumta, P. P. Phule and S. H. Risbud, *Mater. Lett.*, 1987, **5**, 401.
23 Y. Nosaka, N. Ohta and H. Miyama, *J. Phys. Chem.*, 1990, **94**, 3752.
24 P. V. Kamat, N. M. Dimitrijevic and R. W. Fessenden, *J. Phys. Chem.*, 1988, **92**, 2324.
25 S. H. Yu, L. Shu, Y. T. Qian, Y. Xie, J. Yang and L. Yang, *Mater. Res. Bull.*, 1998, **33**, 717.
26 S. H. Yu, L. Shu, Y. S. Wu, J. Yang, Y. Xie and Y. T. Qian, *J. Am. Ceram. Soc.*, 1999, **82**, 457.
27 R. Rosetti, S. Nakahare and L. E. Brus, *J. Chem. Phys.*, 1983, **79**, 1086.
28 F. Williams and A. J. Nozik, *Nature*, 1984, **312**, 21.
29 T. S. Ahmadi, Z. L. Wang, T. C. Green, A. Henglein and M. A. El-Sayed, *Science*, 1996, **272**, 1924.
30 J. Nittmann and H. E. Stanley, *Nature*, 1986, **321**, 663.
31 Y. Zhou, S. H. Yu, C. Y. Wang, X. G. Li, Y. R. Zhu and Z. Y. Chen, *Adv. Mater.*, 1999, **11**, 850.
32 X. F. Qian, Y. Xie and Y. T. Qian, *Mater. Lett.*, 2001, **48**, 109.
33 K. Oikawa, S. Sumi and K. Ishida, *Z, Metallkd.*, 1999, **90**, 13.
34 M. Bredol and J. Merikhi, *J. Mater. Sci.*, 1998, **33**, 471.
35 C. D. Wanger, W. M. Riggs, L. E. Davis, J. F. Moulder and G. E. Muilenberg, *Handbook of X-Ray Photoelectron Spectroscopy*, Perkin-Elmer Corp., Eden Prairie, MN, 1978.
36 I. Nakai, Y. Sugitani, K. Nagashima and Y. Niwa, *J. Inorg. Nucl. Chem.*, 1978, **40**, 789.
37 J. A. Dean, *Lange's Handbook of Chemistry*, McGraw-Hill Book Company, New York, 13th edn., 1972.
38 T. J. Trentler, S. C. Goel, K. M. Hickman, A. M. Viano,

M. Y. Chiary, A. M. Beatly, P. C. Gibbons and W. E. Buhro, *J. Am. Chem. Soc.*, 1997, **119**, 2172.
39 T. J. Trentler, K. M. Hickman, S. C. Goel, A. M. Viano, P. C. Gibbons and W. E. Buhro, *Science*, 1995, **270**, 1791.
40 E. Ben-Jacob and P. Garik, *Nature*, 1990, **343**, 523.
41 Y. Hu, C. V. Rajaram, S. Q. Wang and A. M. Jamieson, *Langmuir*, 1994, **10**, 80.
42 S. Mishra, B. K. Mishra, S. D. Samant, J. Narayanan and C. Manohar, *Langmuir*, 1993, **9**, 2804.
43 J. Herrero and J. Ortega, *Sol. Energy Mater.*, 1988, **17**, 357.